Available online at www.sciencedirect.com
ScienceDirect
Geochimica et Cosmochimica Acta 71 (2007) 5191–5202
Geochimica et Cosmochimica Acta
www.elsevier.com/locate/gca

Solubility of grossular, $Ca_3Al_2Si_3O_{12}$, in H_2O–NaCl solutions at 800 °C and 10 kbar, and the stability of garnet in the system $CaSiO_3$–Al_2O_3–H_2O–NaCl

Robert C. Newton, Craig E. Manning *

Department of Earth and Space Sciences, University of California Los Angeles, Los Angeles, CA 90095-1567, USA

Received 8 February 2007; accepted in revised form 16 August 2007; available online 19 September 2007

Abstract

The solubility and stability of synthetic grossular were determined at 800 °C and 10 kbar in NaCl–H_2O solutions over a large range of salinity. The measurements were made by evaluating the weight losses of grossular, corundum, and wollastonite crystals equilibrated with fluid for up to one week in Pt capsules and a piston-cylinder apparatus. Grossular dissolves congruently over the entire salinity range and displays a large solubility increase of 0.0053 to 0.132 molal $Ca_3Al_2Si_3O_{12}$ with increasing NaCl mole fraction (X_{NaCl}) from 0 to 0.4. There is thus a solubility enhancement 25 times the pure H_2O value over the investigated range, indicating strong solute interaction with NaCl. The $Ca_3Al_2Si_3O_{12}$ mole fraction versus NaCl mole fraction curve has a broad plateau between $X_{NaCl} = 0.2$ and 0.4, indicating that the solute products are hydrous; the enhancement effect of NaCl interaction is eventually overtaken by the destabilizing effect of lowering H_2O activity. In this respect, the solubility behavior of grossular in NaCl solutions is similar to that of corundum and wollastonite. There is a substantial field of stability of grossular at 800 °C and 10 kbar in the system $CaSiO_3$–Al_2O_3–H_2O–NaCl. At high $Al_2O_3/CaSiO_3$ bulk compositions the grossular + fluid field is limited by the appearance of corundum. Zoisite appears metastably with corundum in initially pure H_2O, but disappears once grossular is nucleated. At $X_{NaCl} = 0.3$, however, zoisite is stable with corundum and fluid; this is the only departure from the quaternary system encountered in this study. Corundum solubility is very high in solutions containing both NaCl and $CaSiO_3$: Al_2O_3 molality increases from 0.0013 in initially pure H_2O to near 0.15 at $X_{NaCl} = 0.4$ in $CaSiO_3$-saturated solutions, a >100-fold enhancement. In contrast, addition of Al_2O_3 to wollastonite-saturated NaCl solutions increases $CaSiO_3$ molality by only 12%. This suggests that at high pH (quench pH is 11–12), the stability of solute Ca chloride and Na–Al ± Si complexes account for high Al_2O_3 solubility, and that Ca–Al ± Si complexes are minor. The high solubility and basic dissolution reaction of grossular suggest that Al may be a very mobile component in calcareous rocks in the deep crust and upper mantle when migrating saline solutions are present.

1. INTRODUCTION

Because of its wide stability, compositional variability, and refractory character, garnet is one of the most useful minerals for recording petrologic history of metamorphic rocks. In addition to its great utility in thermobarometry, it is also a sensitive indicator of fluid composition during metasomatic processes. In particular, Ca-rich garnets of the grossular-andradite ($Ca_3Al_2Si_3O_{12}$–$Ca_3Fe_2Si_3O_{12}$) solid-solution series form during fluid–rock interaction in many metamorphic environments, including rodingite alteration of ultramafic rocks (e.g., Evans et al., 1979; Rice, 1983), contact metamorphism of carbonate lithologies (e.g., Einaudi et al., 1981), and regional metamorphism of calc-silicates. These garnets have been used to monitor CO_2 activity (e.g., Warren et al., 1987; Moecher and Essene, 1991) and fO_2 (e.g., Liou, 1974). Replacement of Si^{4+} by a vacancy plus $4H^+$ is a potential monitor of silica activity in

* Corresponding author.
E-mail address: manning@ess.ucla.edu (C.E. Manning).

0016-7037/$ - see front matter © 2007 Elsevier Ltd. All rights reserved.
doi:10.1016/j.gca.2007.08.021

such processes. In addition, fluorine substitution for oxygen in grandite garnets has been used to infer F contents in metamorphic fluids (e.g., Manning and Bird, 1990).

A key to the utilization of calcic garnet in the study of metasomatic processes is knowledge of the solubility of the grossular end member in geologic fluids. The thermodynamic properties of end-member grossular are now well characterized (e.g., Berman, 1988; Holland and Powell, 1998) because experimental work has accurately defined its stability in the system $CaO–Al_2O_3–SiO_2–H_2O$ (Yoder, 1950; Newton, 1966; Huckenholz et al., 1975; Chatterjee et al., 1984). However, these data are not alone sufficient to evaluate the solubility behavior of grossular in complex geologic fluids.

Grossular has relatively low solubility in pure H_2O at 400–800 °C, and up to 10 kbar (Fockenberg et al., 2004). Nevertheless, natural grossular parageneses have been described in which grossular is manifestly of hydrothermal or metasomatic origin, as in the grossular veins in ultramafic rocks at Thetford, Quebec (Westrum et al., 1979). In the absence of large fluid fluxes, it seems likely from these occurrences that the components of grossular may be sufficiently concentrated in natural fluids, either by mutual enhancement or by additional solutes, to cause at least local growth of grossular from a fluid phase.

Grossular may be considered a combination of Al_2O_3 and $CaSiO_3$. Like grossular, the stable forms of these substances, corundum and wollastonite, have low solubility in pure H_2O at pressures (P) and temperatures (T) as high as 10 kbar and 800 °C (Fockenberg et al., 2006; Newton and Manning, 2006; Tropper and Manning, 2007). However, their solubilities are increased by addition of NaCl. Walther (2001a) observed that at 400–600 °C and 0.5–2 kbar, corundum solubility in 0.5 molal (m) NaCl solutions is enhanced by up to 40 times relative to the pure H_2O value. Working at 800 °C, 10 kbar, and to higher NaCl concentrations, Newton and Manning (2006) showed a similar effect, finding that the solubility of corundum was ~10 times higher on a molal basis at $X_{NaCl} = 0.58$ relative to pure H_2O. In both studies, the increase in corundum solubility with NaCl was attributed in part to formation of a $NaAl(OH)_4$ ion pair, consistent with conclusions drawn in some studies of corundum dissolution in NaOH solutions (Barns et al., 1963; Anderson and Burnham, 1967; Pokrovskii and Helgeson, 1995; Diakonov et al., 1996) and $CaCl_2$ solutions (Walther, 2001b). Based on the extent of solubility enhancement at 800 °C, 10 kbar, and the qualitative inference of near-neutral pH (based on near-neutral quench pH), Newton and Manning (2006) proposed that corundum dissolved by a reaction similar to:

$$\underset{\text{corundum}}{Al_2O_3} + Na^+ + 3H_2O = NaAl(OH)_4 + Al(OH)_2^+ \quad (1)$$

Another possible Na–Al species is $NaAlO(OH)_2$, as suggested by Anderson and Burnham (1983).

The solubility of wollastonite at 800 °C and 10 kbar is also enhanced by NaCl (Newton and Manning, 2006). At $X_{NaCl} = 0.3$, wollastonite solubility is 17 times higher than in pure H_2O at the same P and T. Quench pH from these experiments was near 11, qualitatively consistent with OH^- production at high P and T. Based on a simple model in which solute species mix ideally, Newton and Manning (2006) proposed that the simple reaction

$$\underset{\text{wollastonite}}{CaSiO_3} + Na^+ + Cl^- + 2H_2O = CaCl^+ + OH- + H_3NaSiO_4 \quad (2)$$

predominates at all X_{NaCl} and accounts for the solubility enhancement and the high quench pH. The basic solutions generated by wollastonite dissolution in NaCl–H_2O fluids, coupled with Na- and Cl-complexing, may in turn exert a considerable influence on Al_2O_3 mobility and metasomatism involving lime-aluminum silicates such as grossular.

The present study investigates the hydrothermal solubility of grossular at high-grade metamorphic conditions (800 °C and 10 kbar) in the presence of saline fluids. Experiments were designed to investigate whether grossular, like wollastonite and corundum, dissolves congruently in such fluids, whether the large solubility enhancement of the latter minerals in NaCl solutions exists when their components are combined as grossular, and whether saline fluids in the presence of grossular are highly basic, which could have a considerable effect on the metasomatic behavior of other aluminous minerals present. The results give qualitative insight into solute species resulting from grossular dissolution. The study was also designed to investigate the appearance of other possible Ca–Al silicates such as zoisite and anorthite which would indicate departure from the quaternary systems $CaSiO_3–Al_2O_3–H_2O–NaCl$. The results give insight into high-grade metamorphism of siliceous carbonate rocks in the presence of saline fluids.

2. EXPERIMENTAL METHODS

Starting materials were a variety of synthetic and natural minerals placed along with ultrapure H_2O and reagent NaCl in welded Pt tube segments of 3.5 mm diameter and 0.2 mm wall thickness. Synthetic corundum was used in three different forms. Boule chips of 1–5 mg mass were ground into ellipsoids and smoothed with 15 μm diamond paste. Many experiments used polished, 33 mg corundum spheres, as described in Newton and Manning (2006). Electron microprobe analyses of both types of corundum yielded no detectable constituents other than Al_2O_3 (Tropper and Manning, 2007). A third form of corundum was synthetic ultrapure α-Al_2O_3 (Alfa Aesar, lot #H16M55). This material is in the form of fragile hexagonal prisms of length up to 1 mm composed of masses of optically irresolvable, lightly aggregated crystallites (<1 μm), in coherent orientation. The quasi-crystals were ideal starting material in that they could be introduced individually with a needle tip in accurately weighed amounts less than 5 μg.

The $CaSiO_3$ starting material was the very pure natural wollastonite used by Newton and Manning (2006). In $CaSiO_3$-saturated experiments the somewhat fragile wollastonite crystals had to be encapsulated in inner Pt tubes of 0.5 cm length that were crimped at the ends and punctured 2 to 9 times with a needle to allow access of the fluid (Fig. 1a). This procedure allowed determination of the

wollastonite weight loss by weighing the inner capsule before and after an experiment. Wollastonite could also be accurately weighed into a reaction capsule as tiny cleavage fragments (Fig. 1b) on a needle tip.

Several solubility experiments were made with synthetic grossular prepared from stoichiometric $Ca_3Al_2Si_3O_{12}$ glass at 850 °C and 12 kbar. The glass was made by melting a powder of intimately mixed $CaCO_3$, α-Al_2O_3, and ultrapure SiO_2 (quartz, Alpha Aesar) at 1400 °C in a Pt crucible for two hours. The resulting glass was clear and crystal-free. About 40 mg of the glass, introduced as powder or chips, were weighed into a Pt tube segment with about 10 mg H_2O and a tiny seed of natural grossular from Thetford, Quebec. This was the grossular used by Westrum et al. (1979) to measure heat capacity. In one synthesis, the seed grew from 0.9 mg to a dodecahedral crystal of 1.7 mg. In the other synthesis, a 0.1 mg seed grew into a euhedral, translucent 0.4 mg dodecahedron (Fig. 1c). The remainder of the charges recrystallized to coarse, limpid grossular aggregates (Fig. 1d). Both of the single grossular crystals and the aggregates were used as starting material. The cubic unit cell constant was determined by X-ray diffraction scans at 1/2° 2Θ/min with an internal standard of purified annealed corundum. The unit cell constant was 0.1849(1) nm, corresponding to H-free end-member grossular.

The experiments were performed in a 3/4 in. (1.91 cm) diameter piston-cylinder apparatus with NaCl pressure medium and graphite heater sleeve. Approach to run conditions, pressure and temperature monitoring, and quench procedures were as described by (Newton and Manning, 2000, 2005, 2006).

After quenching, the H_2O content of an experiment was redetermined from the drying weight-loss of a quenched capsule and found to agree with the initial H_2O within 0.6 wt%. There was an overall tendency for "H_2O in" to be slightly greater than "H_2O out". This may result from the presence of H_2O in amorphous quench products which could not be entirely dried without endangering the rest of the charge. In some experiments, quench pH measurements were performed on the fluid by puncturing a quenched capsule onto pH paper; in these cases it was not possible to check the H_2O mass balance. Quenched and dried run products were identified and characterized by optical and scanning-electron microscopy. In particular, we searched for any small secondary crystals in the outer capsules which could have resulted from fluid transport across a small temperature gradient (Caciagli and Manning, 2003; Tropper

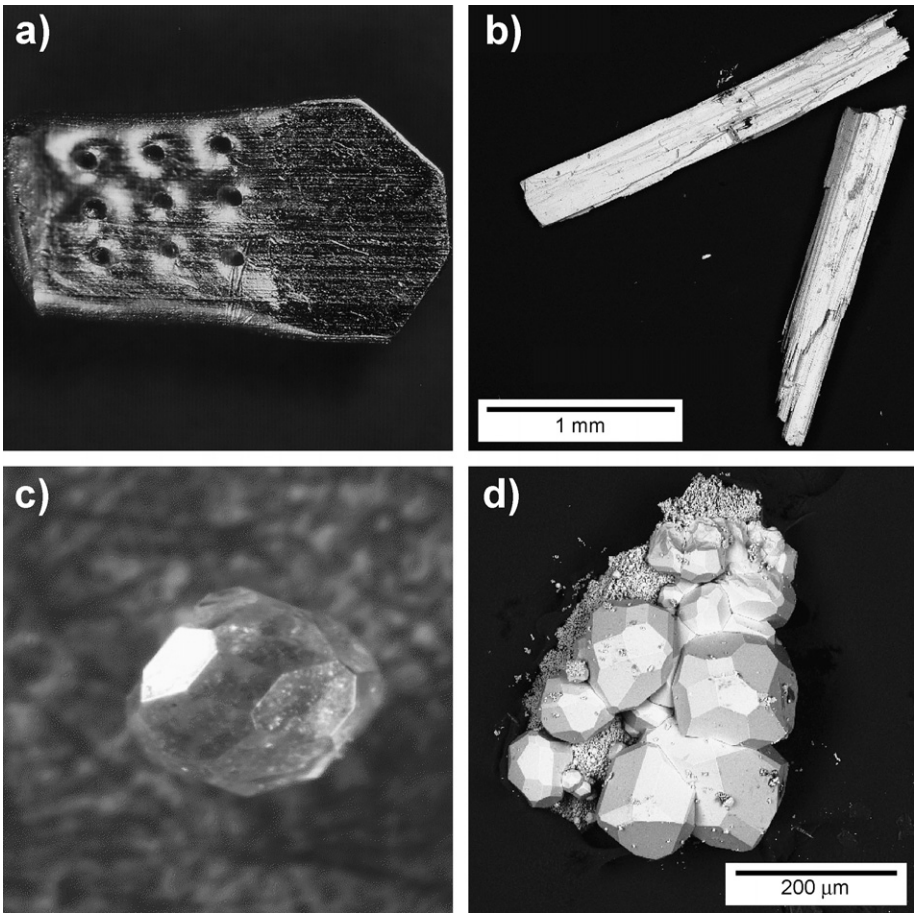

Fig. 1. Back-scattered electron and optical images of starting materials. (a) Pt inner capsule containing wollastonite or grossular starting crystals. Length of capsule is 5 mm. (b) Natural wollastonite crystals. (c) Synthetic garnet single crystal of mass 0.4 mg. (d) Synthetic grossular crystals with minor quench-precipitate material.

and Manning, 2005; Newton and Manning, 2006). Such transport and redeposition could have compromised the solubility measurements based on weight loss. It was usually possible to determine the crystalline run products immediately after drying by low-power binocular microscope observation. Quench halite was removed by rinsing and redrying.

Solubilities were determined by various weight-loss and/or mass-balance methods (see below). H_2O and NaCl weights were determined to a precision of 2 μg (1σ, Mettler M3 microbalance). Changes in weights of solids were with three exceptions determined to higher precision of 0.2 μg (1σ, Mettler UMX2 ultramicrobalance). The starting H_2O weight (Table 1) was used to calculate reported molalities, except for a few cases in which there was partial water loss prior to sealing of the outer capsule. Concentrations of solutes other than NaCl are reported on the molality scale. Uncertainties in solubilities correspond to propagated weighing errors. Concentrations are reported as X_{NaCl} without correction for the negligibly small amounts of other solutes.

3. RESULTS OF EXPERIMENTS

3.1. Quenched run products

Experimental results are given in Table 1. Corundum in most runs with the polished spheres returned as geometrically facetted and etched single crystals, indicative of high solubility (Fig. 2a and b). Boule-chip starting corundum returned with facetted and etch-pitted surfaces indicative of crystallographic control of dissolution and reprecipitation. Run-product corundum produced from fine-grained α-Al_2O_3 occurred as abundant high-refractive-index ($n > 1.8$) hexagonal platelets in run GR-28.

Wollastonite was retrieved in two forms. In $CaSiO_3$-rich runs where wollastonite, with or without garnet, was stable with fluid, one or more residual wollastonite crystals, sometimes with highly irregular shapes, were present in the inner capsules. The other form of wollastonite was a myriad of small, bladed quench-crystals found in both the inner and outer capsules, but only in runs with a bulk composition near wollastonite saturation. In bulk compositions more Al_2O_3-rich than the join grossular-H_2O, quench wollastonite never appeared. Wollastonite was never found to coexist with corundum or zoisite.

Grossular synthesized from initial wollastonite occurred as small (10–20 μm) crystals that could be easily identified optically at low magnification. The presence of grossular was confirmed in oil-immersion mounts under the polarizing microscope. High-index ($n > 1.8$) isotropic dodecahedral crystals typically have cores rich in fluid inclusions and inclusion-free rims. Garnet nucleated and grew as high-index granules on wollastonite crystals enclosed in inner capsules, sometimes forming hollow pseudomorphs of the original wollastonite (Fig. 2c). Careful search indicated that grossular crystals never grew in the outer capsule. Growth in the outer capsule results from small temperature gradients across the charge and would, if it occurred, lead to falsely high solubility estimates from weight loss of encapsulated crystals (Caciagli and Manning, 2003; Tropper and Manning, 2005; Newton and Manning, 2006).

Zoisite grew in Al_2O_3-rich runs at $X_{NaCl} = 0.1$ and 0.3. The zoisite was obvious optically as individual crystals and radiating clusters of slender prisms (Fig. 2d). It was readily recognized in oil-immersion mounts under the polarizing microscope as prismatic crystals with straight extinction and high index of refraction ($n > 1.7$). Zoisite and wollastonite could always be distinguished by their different indices of refraction. No other Ca–Al silicate such as anorthite was found in the quenched charges.

Quench isotropic spherules, or "fish roe", ranging in size from <1 to 10 μm in diameter, were present in every charge. These particles of very low refractive index ($n < 1.5$) were the overwhelming majority of the residue of quenched vapor phase after leaching of the quench halite, and represent the bulk of the fluid phase solutes, apart from NaCl.

A quench pH of 11 to 12 was recorded for all of the fluids tested in which $CaSiO_3$ was present, even at quite low concentrations. Solubility runs on corundum without $CaSiO_3$ gave pH 7 at all salinities, whereas wollastonite solubility experiments without Al_2O_3 gave pH 11 (Newton and Manning, 2006).

3.2. Attainment of equilibrium

All experiments ran for more than 46 h, significantly longer than required to attain constant solubility of corundum or wollastonite (Newton and Manning, 2006). Support for the assumption of equilibrium in most experiments includes time-independence of measurements (e.g., GR-1 and GR-26, Table 1), new crystal facets on corundum, grossular and wollastonite starting crystals despite substantial weight losses, and the observation that corundum and wollastonite never occurred together in run products, in spite of the fact that these minerals, introduced together, were the most frequently used starting material. Reversibility of grossular dissolution was shown by coherence of measurements using both synthetic grossular and metastable starting materials. In these reversal runs, a mixture of fine-grained Al_2O_3 and $CaSiO_3$ on grossular composition yielded grossular syntheses at $Ca_3Al_2Si_3O_{12}$ mole fractions only slightly greater than determined by grossular dissolution experiments. At $X_{NaCl} = 0.1$, metastable zoisite formed in two runs and corundum + fluid persisted in two runs (Table 1 and Fig. 4). These departures from equilibrium can be explained by difficulty of garnet nucleation (see below).

3.3. Solubility of grossular

Grossular dissolves congruently at all NaCl mole fractions from zero to 0.4, as proven by the absence of other crystalline products when only grossular was the crystalline starting material, by the large fluid-only fields (no crystalline products) on the join $Ca_3Al_2Si_3O_{12}$–(H_2O + NaCl), and by our ability to reverse grossular solubility over small compositional intervals from the oversaturated and undersaturated directions at each salinity. One experiment on the natural grossular at $X_{NaCl} = 0.1$ (GR-7, Table 1) gave a

Table 1
Experimental results

Expt	Starting Crystals	Time (hr)	H_2O in (mg)	H_2O out (mg)	NaCl in (mg)	X_{NaCl} in (mg)	Inner capsule in (mg)	Inner capsule out (mg)	Co in (mg)	Co out (mg)	Wo in (mg)	Wo out (mg)	Gr in (mg)	Gr out (mg)	mAl_2O_3	$mCaSiO_3$	Quench pH	Product crystals
GR-39	G_2	68	36.542	36.570	0	0.000	77.0544	76.9641					1.5741	nd	0.0055[b]	0.0165[b]		G
GR-44	G_2	108	36.101	36.151	0	0.000	68.5591	68.4593					0.3412	0.2266	0.0066(03)	0.0198(08)		G
GR-46	G_2	104	36.417	nd	6.224	0.050	69.1651	68.6718					0.6549	0.1470	0.0301	0.0902	11–12	G
GR-9	CW_2	92	36.402	nd	12.902	0.098			32.7205	32.4696	0.4010	0			0.0676	0.0948	11	C
GR-8	CW_1	141	36.702	36.440	13.018	0.099	75.0615	74.3639	0.1025	0	0.8909	0.1358			0.0274	0.1704(39)		W
GR-10	CW_1	91	36.301	36.175	12.908	0.099	75.3803	74.7700	0.0738	0	1.6855	1.0179			0.0199	0.1515(39)		W
GR-3	CW_1	169	30.582	nd	11.063	0.100	69.386	69.040	1.424	0.988	0.895	0			*0.100*	*0.132*	11–12	GC
GR-4	CW_1	166	33.419	33.318	12.102	0.100	81.185	80.711	2.122	1.687	0.784	0			*0.107*	*0.140*		GC
GR-12	CW_1	84	37.721	nd	13.590	0.100	86.5921	85.8296	0.1838	0	1.8916	nd			<0.0478	<0.1740	11	GW
GR-15	CW_1	89	35.585	35.609	12.811	0.100	79.4870	78.8880	0.1427	0	1.7885	nd			<0.0393	>0.1449		GW
GR-17	CW_2	76	35.981	35.364	12.980	0.100			0.1862	0	0.6353	0			0.0508	0.1520		—
GR-18	CW_2	46	35.626	35.628	12.848	0.100			0.1911	0	0.6717	0			<0.0526	<0.1623		G
GR-19	CW_2	97	32.914	nd	11.867	0.100			32.9178	32.5381	0.6545	0			0.1131	0.1712	11	C
GR-20	CW_2	93	35.968	35.956	12.978	0.100			0.2898	0	0.6937	0			<0.0790	<0.1660		G
GR-21	CW_2	92	36.178	36.079	13.049	0.100			32.6617	32.1541	0.8380	0			<0.1376	<0.1994		CZ
GR-22	CW_2	92	35.975	35.851	12.972	0.100			0.3361	0	0.6708	0			<0.0916	<0.1605		G
GR-23	CW_2	68	37.106	nd	13.381	0.100			32.8135	32.6969	0.1248	0			0.0308	0.0290	11	C
GR-24	CW_2	98	36.326	nd	13.101	0.100			0.4564	nd	0.7611	0			<0.1232	<0.1804		CZ
GR-37	CW_2G_2	78	24.893	24.959	8.985	0.100	81.0999	81.0560	0.1139	0	0.3716	0	1.6622	1.5754	0.0507(11)	0.1460(33)		G
GR-38	CG_1	115	24.994	24.521[a]	9.015	0.100			0.0888	0			0.4850	0	0.0794	0.1317		—
GR-11	CW_2	92	36.639	36.622	13.290	0.101			32.7025	32.3605	0.5649	0			0.0915	0.1327		C
GR-16	CW_2	69	37.480	nd	13.598	0.101			0.2104	0	0.7446	0			<0.0551	<0.1710	11	G
GR-6	CW_1	165	33.056	nd	12.244	0.102	75.559	75.073	0.266	0	1.640	0.492			*0.0345*	*0.166*	11–12	GW
GR-7	G_1	166	35.516	nd	13.040	0.102							20.389	19.423	0.0604	0.1811	11	G
GR-14	CW_2	92	nd	34.208	12.563	0.102			32.8175	32.6353	0.2272	0			0.0522	0.0572		C
GR-13	CW_2	94	36.832	nd	14.158	0.106			32.6338	32.2281	0.6810	0			0.1080	0.1592	11–12	C
GR-30	CW_2	189	30.356	30.315	24.625	0.200			0.2535	0	0.7915	0			0.0819	0.2245		—
GR-40	CW_2G_2	91	25.074	24.997	20.338	0.200	72.3399	72.2335	0.1835	0	0.5775	0	1.4678	1.2605	0.0857(26)	0.2399(77)		G
GR-34	CW_2	72	23.626	23.693	32.756	0.299			0.2445	0	0.8458	0			<0.1015	<0.3082		G
GR-25	CW_2	96	29.039	nd	40.433	0.300			0.2963	0	1.0021	0			0.1001	0.2971	11	—
GR-27	CW_1	89	25.067	25.196	34.833	0.300	81.4710	80.7117	0.1281	0	3.7458	2.8429			0.0501	0.3101		W
GR-28	CW_1	168	26.135	26.041	36.355	0.300	85.2395	84.2566	0.1856	0	3.0465	nd			<0.0696	>0.3238		GW
GR-29	CW_2	96	23.001	22.901	31.959	0.300			32.5734	32.1897	0.7902	0			<0.1636	<0.2957		CZ
GR-31	CW_2	96	26.008	25.856	36.179	0.300			32.6744	32.1063	1.0679	0			<0.2142	<0.3535		CZ
GR-32	CW_2	94	26.963	26.892	37.531	0.300			0.2654	0	0.8705	0			0.0965	0.2779		—
GR-33	CW_2	93	25.110	24.998	34.857	0.300			32.6667	32.2157	0.9126	0			<0.1762	<0.3129		CZ
GR-35	CW_2	78	26.059	25.997	36.254	0.300			2.0442	1.6090	0.8346	0			0.1638	0.2757		C
GR-42	G_2	92	20.002	nd	27.822	0.300	66.1016	65.2463					1.9168	0.9762	0.0997(27)	0.2990(82)		G
GR-43	CG_2		20.047	19.914	27.860	0.300	77.0599	76.3345	1.0851	0.9177			0.9156	0	<0.1833	<0.3042		CZ
GR-26	CW_2	111	nd	28.036	41.133	0.311			32.6564	32.2869	0.8033	0			0.1293	0.2467		C

(*continued on next page*)

Table 1 (*continued*)

Expt	Starting Crystals	Time (hr)	H_2O in (mg)	H_2O out (mg)	NaCl in (mg)	X_{NaCl} in (mg)	Inner capsule in (mg)	Inner capsule out (mg)	Co in (mg)	Co out (mg)	Wo in (mg)	Wo out (mg)	Gr in (mg)	Gr out (mg)	mAl_2O_3	$mCaSiO_3$	Quench pH	Product crystals
GR-1	CW_1	66	nd	32.361	47.921	0.313	71.957	71.54	1.952	1.473	0.922	0			0.145	0.245		C
GR-45	CW_2	87	19.052	18.969	41.236	0.400			0.2407	0	0.7899	0			0.1239	0.3569		—
GR-47	CW_2	89	19.032	19.063	41.116	0.400			0.2605	0	0.8847	0			<0.1342	<0.4002		G
GR-48	CW_2G_2	85	19.983	19.863	43.261	0.400	84.8313	84.6970	0.2206	0	0.7324	0	0.6067	0.3920	0.1321	0.3894		G

Explanation: "in", denotes weight prior to experiment; "out," after; "nd," not determined. Key to starting materials: C, synthetic corundum; G_1, natural grossular; G_2 synthetic grossular; W_1, natural wollastonite in inner capsule; W_2, unencapsulated natural wollastonite. Key to product crystals: C, corundum; G, grossular; W, wollastonite; Z, zoisite; —, none. Calculated molalities (*m*) of Al_2O_3 and $CaSiO_3$ are given to three or four decimal places, depending on balance used in weighing inner capsule and/or crystals (see text). Corresponding 1σ uncertainties propagated from 2 and 0.2 μg weighing errors are 0.001 and 0.0001 molal, respectively, unless molality value is followed by a parenthetical entry, which gives 1σ uncertainty in last digits. These larger errors arise when weight loss of crystal(s) and inner capsule were averaged (underlined entries; see text). Italics indicate molality calculated by mass balance (see Appendix A). Experiments in which results provide only a minimum or maximum solubility constraint are preceded by "<" or ">" symbols (see text).

[a] Indicates H_2O out used to calculate molality.

[b] Indicates inner-capsule weight change used to calculate molality.

slightly higher solubility than results on synthetic crystals (GR-37). This is likely due to presence of other elements in this material. Fig. 3 shows grossular solubility as a function of NaCl mole fraction based on the six weight-loss experiments on synthetic grossular only at 800 °C and 10 kbar. The grossular molality (m_{gr}) data were fit to the equation $m_{gr} = 0.00755 + 0.439X_{NaCl} - 0.343X^2_{NaCl}$ ($R = 0.996$) (Fig. 3). A great enhancement of solubility at high salinity is evident: molality increases by a factor of 25 over the salinity range studied.

3.4. Equilibrium phase relations in the system $CaSiO_3$–Al_2O_3–H_2O–NaCl

The results permit derivation of the fluid stability field and approximate phase boundaries as functions of Al_2O_3, $CaSiO_3$ and NaCl concentrations in the fluid (Fig. 4). Locations of the phase boundaries for each assemblage were determined independently based on the nature of the solubility determination, as described below. It must be emphasized that Fig. 4 is largely a synthesis diagram; the phases produced in the syntheses were generally consistent with the results from our weight-loss experiments (mainly on grossular and corundum).

3.4.1. Corundum + fluid boundary

Points on the corundum + fluid boundary were directly determined from the weight loss of a corundum sphere or boule chip. In corundum-present runs at $X_{NaCl} = 0.1$ where $CaSiO_3$ was not encapsulated (Table 1), the corundum + fluid boundary was terminated by the appearance of zoisite (Fig. 4). However, when the wollastonite was introduced as a large encapsulated single crystal, the dissolution behavior was quite different. The wollastonite crystal was pseudomorphed by granular grossular (Fig. 2c) at a considerably smaller $m_{Al_2O_3}$ than for the first appearance of zoisite, which proves that grossular is the stable synthesis product of Al_2O_3 and $CaSiO_3$ at this salinity, and that zoisite is a metastable synthesis product when grossular is inhibited. Apparently, wollastonite is able to nucleate grossular, and, in runs where all of the initial wollastonite quickly dissolves, garnet fails to nucleate at its equilibrium solubility limit in Al_2O_3-rich bulk compositions, but is metastably overstepped in favor of the more aluminous phase zoisite. Two runs at $X_{NaCl} \approx 0.3$ yielded disparate results (GR-1 and GR-26) for corundum solubility; in both cases, H_2O-in weight could not be measured because of water loss prior to sealing the outer capsule, and H_2O balance could not be demonstrated.

3.4.2. Wollastonite + fluid boundary

The extent of wollastonite dissolution was usually determined by weight loss of the inner capsule, after removal of the quench halite by repeated soaking in water and drying, until constant weight was obtained. This method consistently underestimates the $CaSiO_3$ content of the fluid because of insoluble quench material remaining in the inner capsule. In a few charges an irregularly shaped residual wollastonite crystal could be extracted whole and weighed.

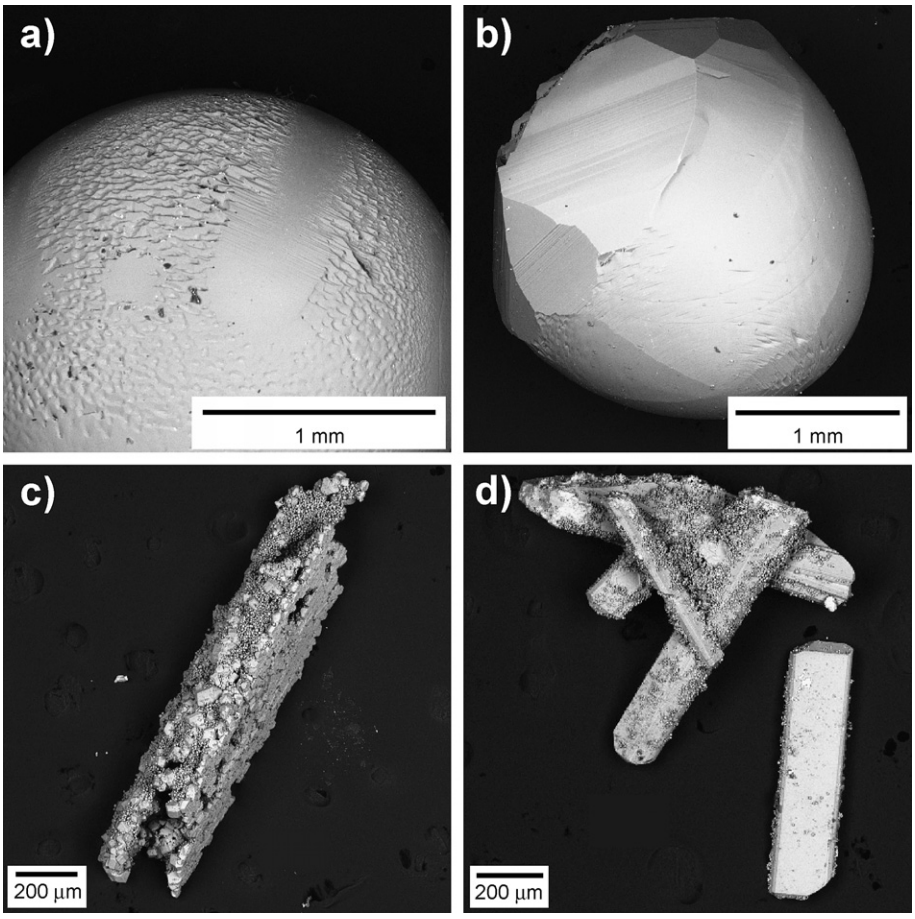

Fig. 2. Back-scattered electron images of run products. (a) Slightly dissolved corundum sphere showing etch pits. (b) Substantially dissolved corundum former sphere with large new facets. (c) Pseudomorph of granular garnet replacing former wollastonite starting crystal. Some fine-grained quench material present. (d) Zoisite crystals formed by reaction of original grossular and corundum with fluid at $X_{NaCl} = 0.3$. Fine quench-material coats crystals.

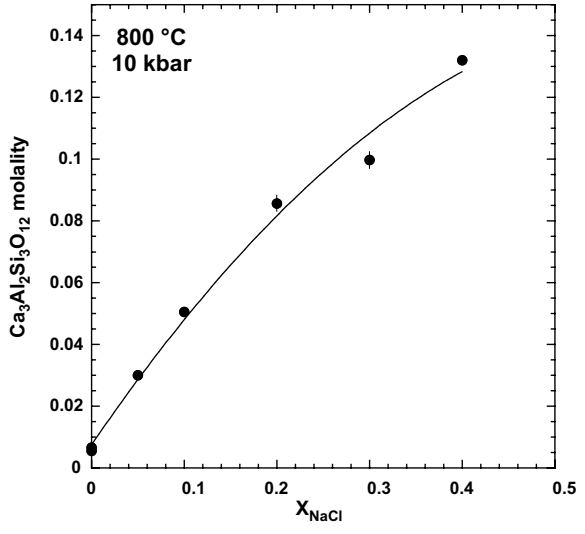

Fig. 3. Variation in grossular molality (moles $Ca_3Al_2Si_3O_{12}$/kg H_2O) with NaCl mole fraction at 800 °C and 10 kbar. The solid line shows the fitted curve: $m_{gr} = 0.00755 + 0.439X_{NaCl} - 0.343X^2_{NaCl}$ ($R = 0.996$).

The weight loss of a wollastonite crystal may be considered to yield a maximum solubility value because of the fragile nature of the crystals, which could have resulted in slight breakage loss. In these runs, the average of the crystal weight loss and the inner-capsule weight loss (Table 1) was used to calculate the solubility (Fig. 4).

3.4.3. *Grossular + fluid boundary*

Upper limits for the concentration of solutes in the field grossular + fluid were determined by synthesis experiments from fine-grained $Al_2O_3 + CaSiO_3$ on or near grossular bulk composition which yielded grossular, and lower limits were determined from similar experiments which failed to produce any crystals. The bulk compositions of these runs are plotted as phase diagram constraints in Fig. 4. For synthesis-type runs in which fine-grained grossular was produced, the fluid composition data in Table 1 are prefixed by "<". Absolute determinations of the solubility of grossular at $X_{NaCl} = 0$, 0.05, 0.1, 0.2, 0.3, and 0.4 were based on weight losses of the synthetic grossular crystals in runs Gr-39 and 44, 46, 37, 40, 42, and 48, respectively.

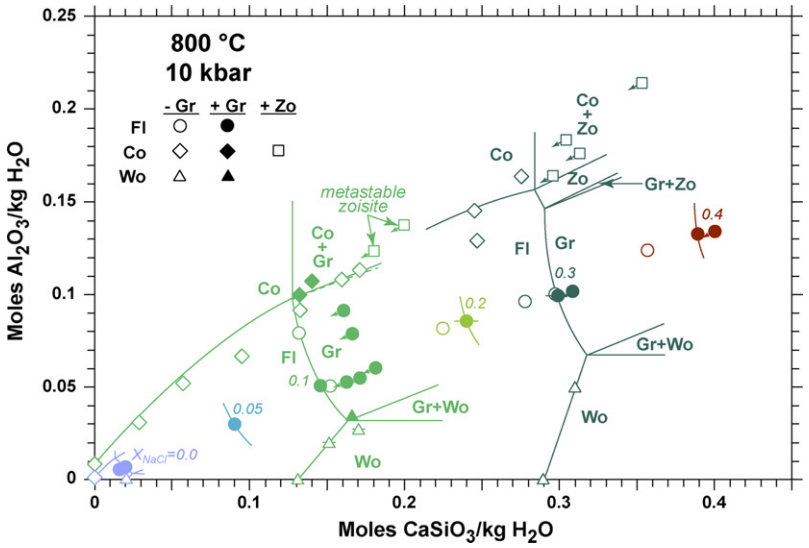

Fig. 4. Compositions of solutions coexisting with various crystalline assemblages and phase assemblage boundaries in the system Al_2O_3–$CaSiO_3$–H_2O–NaCl at 800 °C and 10 kbar. Axis labels refer to the bulk compositions of starting materials. Phase boundaries were sketched to optimize consistency with observed product assemblages although minor inconsistencies are evident (see text). Solid lines denote stable phase boundaries; dashed lines, metastable extensions. Plotted points represent fluid composition only in the fields without crystalline product phases. Grossular-bearing assemblages are denoted with filled symbols. Phase relations involving zoisite are slightly off the Al_2O_3–$CaSiO_3$–H_2O compositional plane. Arrows indicate direction to relevant phase boundary in experiments providing a maximum solubility constraint. Abbreviations: Co, corundum; Fl, fluid; Gr, grossular; Wo, wollastonite; Zo, zoisite.

3.4.4. Grossular + corundum + fluid invariant point

The assemblage grossular + corundum + fluid is, at fixed T, P, and X_{NaCl}, invariant. The composition of this invariant fluid at $X_{NaCl} = 0.1$ could be determined by mass balance from the weight losses of the corundum crystal and the inner capsules (see Appendix A), based on runs GR-3 and GR-4 (Table 1). In two experiments at $X_{NaCl} = 0.1$ starting with fine-grained Al_2O_3 and unencapsulated $CaSiO_3$ (GR-21 and GR-24, Table 1), a synthesis of corundum and zoisite was obtained. Inasmuch as there was no way to determine the absolute amounts of zoisite or corundum produced, the starting bulk compositions are plotted in Fig. 4 as merely phase-diagram constraints (in this case, metastable points).

3.4.5. Zoisite + corundum + fluid invariant point

Zoisite was persistently produced in runs with large corundum crystals at $X_{NaCl} = 0.3$. The assemblage zoisite+ corundum+ fluid was proven to be stable relative to the assemblage grossular + corundum + fluid by run GR-43, Table 1, in which the starting crystals were corundum and synthetic grossular. The run yielded abundant zoisite, and the grossular entirely disappeared. The zoisite composition does not lie in the plane $CaSiO_3$–Al_2O_3–H_2O–NaCl; this is the only departure from the quaternary system which was observed in crystalline products of the present study.

3.4.6. Wollastonite + grossular + fluid invariant point

The fluid composition of the invariant assemblage wollastonite + grossular + fluid could not be determined directly because the amount of grossular produced could not be determined absolutely. The runs yielding this assemblage are plotted in Fig. 4 as phase-diagram constraints. These points, together with constraints on the other phase fields and lines, serve to determine the wollastonite–grossular–fluid invariant point approximately.

3.4.7. Additional considerations

Phase boundaries in Fig. 4 were constructed to be consistent with the measured points, the constraining points,

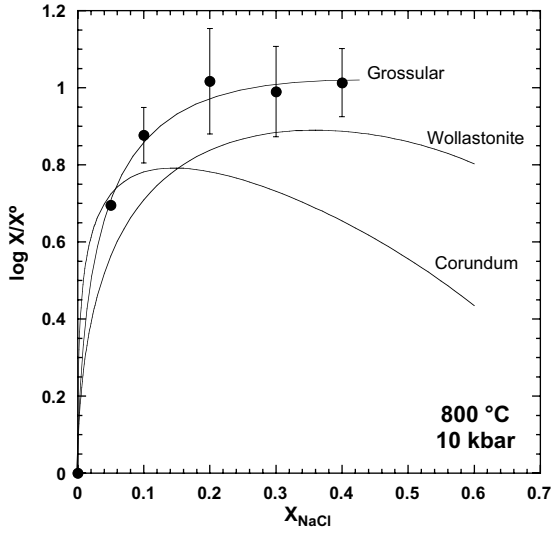

Fig. 5. Solubility enhancement of corundum, wollastonite and grossular in NaCl–H_2O solutions at 800 °C and 10 kbar, expressed as the logarithm of the ratio of the mole fraction at a given NaCl concentration to that in pure H_2O (X/X°). Data for corundum and wollastonite are from Newton and Manning (2006). Grossular mole fraction calculated assuming complete dissociation of NaCl, as described by Newton and Manning (2006).

and phase-equilibrium constraints on the locations of metastable extensions. Boundaries emanating from 3-phase points must be straight lines projecting to the stoichiometric compositions of the phases (Al_2O_3, $CaSiO_3$, and $Ca_3Al_2Si_3O_{12}$). In Cartesian coordinates, the slopes of lines bounding three-phase fields are infinite, 1/3 and zero. Locations of the phase boundaries were drawn to minimize minor contradictions in the data. It is important to note that invariant points are generally not closely constrained by the synthesis and weight-change data.

Key features revealed by Fig. 4 are (1) the congruency of grossular solubility on its own composition in the join $CaSiO_3$–Al_2O_3 up to at least $X_{NaCl} = 0.4$, and (2) the great enhancement of grossular solubility by the presence of NaCl, such that grossular molality increases ~25-fold from $X_{NaCl} = 0$ to $X_{NaCl} = 0.4$. In addition, there is very great enhancement of corundum solubility by the combination of NaCl and $CaSiO_3$. Fig. 4 shows that corundum solubility increases about 130-fold from $X_{NaCl} = 0$ to zoisite saturation at $X_{NaCl} = 0.3$. It is also evident that corundum solubility is enhanced by the presence of $CaSiO_3$ along with NaCl in solution, and that Al_2O_3 solubility dependence on NaCl occurs mainly because of the large effect of NaCl on $CaSiO_3$ solubility. In contrast, the effect of solute Al_2O_3 on wollastonite solubility is quite small (only about 12% increase before grossular saturation at $X_{NaCl} = 0.4$).

4. DISCUSSION

4.1. Solubility enhancement

Fig. 5 shows the relative solubility enhancement of grossular, corundum and wollastonite in NaCl–H_2O solutions, expressed as $\log(X_i/X_i^\circ)$, where X_i° is the mole fraction of congruently dissolving mineral i in initially pure H_2O. At high X_{NaCl}, grossular shows greater relative solubility enhancement than wollastonite or corundum. Corundum and wollastonite show well-defined maxima at $X_{NaCl} = 0.14$ and 0.33, respectively. The relative solubility enhancement of grossular also flattens markedly above $X_{NaCl} = 0.2$. This results from two competing factors: complexing in solution, which initially enhances solubility, and progressive destabilization of hydrous species as H_2O activity decreases with increasing salinity (Newton and Manning, 2006). The maximum for corundum at low NaCl mole fraction implies that the dominant alumina solute is relatively more hydrous than the solute lime and silica species in the subsystems bounding grossular-H_2O–NaCl.

4.2. Dissolution mechanisms

Grossular may be considered as a compound of the components Al_2O_3 and $CaSiO_3$. It is of interest to assess whether the solution characteristics of these compounds individually may provide some prediction of their mutual solubility and speciation in the dissolution of grossular. The model dissolution reactions, Eqs. (1) and (2), may be used as a starting point, along with the inference that the flatness of the grossular dissolution curve (Fig. 5) suggests that a maximum may occur somewhere in the range $0.25 \leqslant X_{NaCl} \leqslant 0.5$, though the present data do not define this feature. This possibility suggests a molar ratio of NaCl:H_2O in the grossular dissolution reaction of between 1:1 and 1:3.

In Eqs. (1) and (2), $NaAl(OH)_4$ results from corundum dissolution, and H_3NaSiO_4 from wollastonite dissolution. These species would probably react to some extent to produce Na–Al–Si species, most likely as neutral hydrous molecules (Anderson and Burnham, 1983). A plausible Al–Si species is $NaAlSiO(OH)_6$, analogous to the dimeric species $Si_2O(OH)_6$ and $AlSiO(OH)_5$ which are inferred to be abundant in aqueous solutions at high P and T (Newton and Manning, 2002, 2003; Manning, 2007). Another possibility might be solute molecules having nearly albite stoichiometry.

If neutral Na–Al–Si species form, they will consume Na at the expense of Cl, which will be available to complex with Ca^{+2}. Newton and Manning (2006) proposed that $CaCl^+$ was the dominant species with wollastonite. This is consistent with extrapolated $CaCl_2$ and HCl dissociation constants (Frantz and Marshall, 1982, 1984a,b) and H_2O ionization constants (Marshall and Franck, 1981), which indicate that $CaCl^+$ is the predominant Ca species at moderate to high total chloride at 800 °C, 10 kbar, when total Ca molality is equal to that of the Cl left uncompensated by formation of H_3NaSiO_4. Ca–Al ± Si species can be discounted in favor of more stable Na–Al ± Si species because the addition of solute Al_2O_3 to NaCl produces only slight additional enhancement of $CaSiO_3$ solubility.

A final consideration is that OH^- can be inferred to be a product of the grossular dissolution reaction because of the high pH of the quenched fluids. This is sensible because if $CaCl^+$ and H_3NaSiO_4 predominate, OH– must be produced in the dissolution reaction to maintain electrical neutrality. An alternative possibility for producing high quench pH might be the inversion of solute H_3NaSiO_4 to NaOH and H_4SiO_4 during or after the quench; however, Newton and Manning (2006) found neutral quenched fluid from solubility experiments at 800 °C and 10 kbar on quartz in H_2O–NaCl solutions. Because of the likelihood of forming of Ca chloride in the present experiments, we regard it as more probable that the cause of high pH results from dissolution of lime minerals in NaCl solutions rather than quench dissociation.

The above considerations are, when taken together, restrictive, and imply a limited number of possible controlling dissolution reactions. One not necessarily unique possibility which takes into account the above criteria is:

$$\underset{\text{grossular}}{Ca_3Al_2Si_3O_{12}} + 3Na^+ + 3Cl^- + 9H_2O = 3CaCl^+ + 2NaAlSiO(OH)_6 + 3OH^- + H_3NaSiO_4 \quad (3)$$

The high degree of hydration of the postulated solute species would account for the marked flattening of the grossular dissolution curve in Fig. 5.

4.3. Large enhancement of corundum solubility

The combination of NaCl and $CaSiO_3$ in solution increases the molality of Al_2O_3 in equilibrium with corundum

by a factor of nearly 130 over that in initially pure H_2O, and of ~10 relative to that in $CaSiO_3$-free H_2O–NaCl fluids (Fig. 4). This strongly suggests that the controlling factor is the great enhancement of $CaSiO_3$ dissolution with NaCl, producing $CaCl^+$, which, in turn, produces OH^-. The OH^--enhanced solubility of corundum is limited by the appearance of grossular.

4.4. Zoisite stability

The appearance of zoisite in H_2O–NaCl fluids at high X_{NaCl} might seem counter-intuitive, inasmuch as zoisite is a hydrate. However, other factors which stabilize zoisite, particularly Al_2O_3 content of the fluid, increase with NaCl. Grossular and corundum react with fluid at X_{NaCl} somewhere between 0.1 and 0.3 to produce stable zoisite. The early metastable appearance of zoisite at $X_{NaCl} = 0.1$ occurs because the limiting Al_2O_3 content of the fluid in equilibrium with grossular is overstepped in the absence of grossular seeds until zoisite becomes saturated.

4.5. Geological applications

Grossular garnet is much more soluble in NaCl–H_2O fluids than in Cl-free H_2O at high P and T, and moreover, shows simple congruent dissolution in these fluids. A first-order deduction is that small amounts of brines infiltrated into deep-crust sequences containing calcareous rocks may effect substantial mobilization of Al_2O_3, a component commonly assumed to be an inert reference substance on which to base mass-transfer calculations (e.g., Carmichael, 1969).

An unknown factor is the additional effect of CO_2 as limestone is converted to calc-silicate assemblages. This is an unfortunate consideration which is not addressed in the present study, one which limits attempted applications. Thompson (1975) described a zone of metasomatic interaction between a marble and an aluminous metasedimentary rock in Vermont. A one-meter interval between the contrasting rock types is variably enriched in CaO and Al_2O_3, with an intermediate zone of nearly monomineralic grossular, where the Al_2O_3 content is higher than in the source rocks (the metapelites). Thompson's (1975) attempt to model the chemical profile across the contact as a diffusion gradient yielded inconclusive results. The present experimental results support an alternative hypothesis. The lithologic contrast may have been a conduit for the infiltration of fluids (e.g., Ferry, 1992; Léger and Ferry, 1993), which, if saline, could have induced appreciable mobility of alumina. In general, some modern estimates of metasomatism in regional metamorphism have concluded that bulk chemical changes may have been much greater than formerly anticipated (Ague, 1994). The present work indicates that some chemical changes in rocks undergoing regional metamorphism may be greatly enhanced in some components, particularly those of low solubility in nearly pure H_2O, if the fluids involved have significant salt content.

The principal mechanism of Al_2O_3 mobilization in saline fluids at elevated P and T appears to be the high solubility of lime silicates in such fluids, with consequent generation of high pH, which, in turn favors the formation of solute Na–Al–(Si) complexes. The maximum solubilities of Al-species occur in the concentrated brine range corresponding to mole fractions of NaCl between 0.2 and 0.4. This is significant because such fluids have anomalously low H_2O activity (Aranovich and Newton, 1996); thus they inhibit rock melting at high fluid pressures, even at temperatures of 800 °C or more. Small amounts of pore fluids may, if they are concentrated brines, have disproportionate effects on chemical migration in the deep crust and upper mantle.

ACKNOWLEDGMENTS

This research was supported by a U.S. National Science Foundation Grant EAR-033717. We thank Cam Macris and Frank Kyte for help in the microscopic imaging, and Wayne Dollase, Alan Thompson, and Peter Tropper for stimulating and helpful discussions. Eric Essene supplied the natural grossular sample. The manuscript was improved by critical comments of T. Chacko, W. Maresch, J. Walther, and an anonymous reviewer.

APPENDIX A

Solute concentrations are mostly based on mass losses of starting material crystals in this study. In cases where new phases appear and grow by reactions with the fluid, it may be difficult or impossible to use a direct crystal mass-loss technique. This is true if a new phase is nucleated on a starting phase so that it is impossible to separate the new phase and weigh it. Additionally, it may be impossible to reclaim with confidence all of the new phase if it is in the form of dispersed small grains, even if the starting phase it replaces is completely consumed. The use of a weighable inner capsule which contains one of the starting phases, and in which it may be assumed with confidence that the new reaction phase is completely contained, circumvents the dispersed product-phase problem. In this case, three mass balance equations may be written:

$$\text{weight loss corundum} = \text{weight dissolved } Al_2O_3 + 0.2264 \times \text{weight grossular} \quad (A1)$$

$$\text{weight loss wollastonite} = \text{weight dissolved } CaSiO_3 + 0.7736 \times \text{weight grossular} \quad (A2)$$

$$\text{weight loss inner capsule} = \text{weight dissolved } CaSiO_3 - 0.2264 \times \text{weight grossular} \quad (A3)$$

Elimination of the (unknown) weight of grossular gives:

$$\text{weight dissolved } CaSiO_3 = 0.2264 \text{ weight loss wollastonite} + 0.7736 \times \text{weight loss inner capsule} \quad (A4)$$

$$\text{weight dissolved } Al_2O_3 = \text{weight loss inner capsule} + \text{weight loss corundum} - \text{weight dissolved } CaSiO_3 \quad (A5)$$

Determination of the concentrations of dissolved $CaSiO_3$ and Al_2O_3 in Experiment GR-4, Table 1, serves as an example. The crystalline starting material was a large

corundum crystal and a large encapsulated wollastonite crystal. The products were a smaller corundum crystal and a quantity of small grossular crystals, all contained in the inner capsule, but impossible to collect and weigh separately. The measured quantities were the weight changes of the corundum crystal and of the inner capsule. The weight loss of wollastonite is the entire amount originally introduced, since it disappeared entirely. The data give dissolved $CaSiO_3$ and Al_2O_3 weights of 0.544 and 0.345 mg, respectively, leading to $m_{CaSiO_3} = 0.140$ and $m_{Al_2O_3} = 0.107$, which together define the invariant fluid composition at $X_{NaCl} = 0.1$ in equilibrium with grossular and corundum.

REFERENCES

Ague J. J. (1994) Mass transfer during Barrovian metamorphism of pelites, south-central Connecticut. II. Channelized fluid flow and the growth of staurolite and kyanite. *Am. J. Sci.* **294**, 1061–1134.

Anderson G. M. and Burnham C. W. (1967) Reaction of quartz and corundum with aqueous chloride and hydroxide solutions at high temperatures and pressures. *Am. J. Sci.* **265**, 12–27.

Anderson G. M. and Burnham C. W. (1983) Feldspar solubility and the transport of aluminum under metamorphic conditions. *Am. J. Sci.*, 283–297.

Aranovich L. Y. and Newton R. C. (1996) H_2O activity in concentrated NaCl solutions at high pressures and temperatures measured by the brucite-periclase equilibrium. *Contrib. Mineral. Petrol.* **125**, 200–212.

Barns R. L., Laudise R. A. and Shields R. M. (1963) The solubility of corundum in basic hydrothermal solvents. *J. Phys. Chem.* **67**, 835–839.

Berman R. G. (1988) Internally consistent thermodynamic data for minerals in the system Na_2O–K_2O–CaO–MgO–FeO–Fe_2O_3–Al_2O_3–SiO_2–TiO_2–H_2O–CO_2. *J. Petrol.* **29**, 445–522.

Caciagli N. C. and Manning C. E. (2003) The solubility of calcite in water at 5–16 kbar and 500–800 °C. *Contrib. Mineral. Petrol.* **146**, 275–285.

Carmichael D. M. (1969) On the mechanism of prograde metamorphic reactions in quartz-bearing pelitic rocks. *Contrib. Mineral. Petrol.* **20**, 244–267.

Chatterjee N. D., Johannes W. and Leistner H. (1984) The system CaO–Al_2O_3–SiO_2–H_2O: new equilibrium data, calculated phase relations, and their petrological applications. *Contrib. Mineral. Petrol.* **88**, 1–13.

Diakonov I., Pokrovski G., Schott J., Castet S. and Grout R. (1996) An experimental and computational study of sodium–aluminum complexing in crustal fluids. *Geochim. Cosmochim. Acta* **60**, 197–211.

Einaudi M. T., Meinert L. D. and Newberry R. J. (1981) Skarn deposits. *Econ. Geol.* **75th Anniversary Volume**, 317–391.

Ferry J. M. (1992) Regional metamorphism of the Waiats River Formation, eastern Vermont: delineation of a new type of giant metamorphic hydrothermal system. *J. Petrol.* **33**, 45–94.

Fockenberg T., Burchard M. and Maresch W. V. (2004) Solubilities of calcium silicates at high pressures and temperatures. *Lithos* **73**, S37.

Fockenberg T., Burchard M. and Maresch W. V. (2006) Experimental determination of the solubility of natural wollastonite in pure water up to pressures of 5 GPa and at temperatures of 400–800 °C. *Geochim. Cosmochim. Acta* **70**, 1796–1806.

Evans B. W., Trommsdorf V. and Richter W. (1979) Petrology of an eclogite–metarodingite suite at Cimi di Gagnone, Ticino, Switzerland. *Am. Mineral.* **64**, 15–31.

Frantz J. D. and Marshall W. L. (1984a) Electrical conductances and ionization constants of salts, acids and bases in supercritical aqueous fluids: 1. hydrochloric acid from 100° to 700 °C and at pressures to 4000 bars. *Am. J. Sci.* **284**, 651–667.

Frantz J. D. and Marshall W. L. (1984b) Electrical conductances and ionization constants of calcium chloride and magnesium chloride in aqueous solutions at temperatures to 600 °C and pressures to 4000 bars. *Am. J. Sci.* **282**, 1666–1693.

Holland T. J. B. and Powell R. (1998) An internally consistent thermodynamic data set for phases of petrologic interest. *J. Metamorph. Geol.* **16**, 309–343.

Huckenholz H. G., Holzl E. and Lindhuber W. (1975) Grossularite, its solidus and liquidus relations in the CaO–Al_2O_3–SiO_2–H_2O system up to 10 kbar. *Neues Jb. Miner. Abh.* **124**, 1–46.

Léger A. and Ferry J. M. (1993) Fluid infiltration and regional metamorphism of the Waits River Formation, north-east Vermont, USA. *J. Metamorph. Geol.* **11**, 3–29.

Liou J. G. (1974) Stability relations of andradite-quartz in the system Ca–Fe–Si–O–H. *Am. Mineral.* **59**, 1016–1025.

Manning C. E. and Bird D. K. (1990) Fluorian garnets from the host rocks of the Skaergaard intrusion: implications for metamorphic fluid composition. *Am. Mineral.* **75**, 859–873.

Manning C. E. (2007) Solubility of corundum + kyanite in H_2O at 700 °C and 10 kbar: evidence for Al–Si complexing at high pressure and temperature. *Geofluids* **7**, 258–269.

Marshall W. L. and Franck E. U. (1981) Ion product of water substance, 0–1000 °C, 1–10,000 bars: new international formulation and its background. *J. Phys. Chem. Ref. Data* **10**, 295–304.

Moecher D. P. and Essene E. J. (1991) Calculation of CO_2 activities using scapolite equilibria: constraints on the presence and composition of a fluid phase during high grade metamorphism. *Contrib. Mineral. Petrol.* **108**, 219–240.

Newton R. C. (1966) Some calc-silicate equilibrium relations. *Am. J. Sci.* **264**, 204–222.

Newton R. C. and Manning C. E. (2000) Quartz solubility in H_2O–NaCl and H_2O–CO_2 solutions at deep crust-upper mantle pressures and temperatures: 2–15 kbar and 500–900 °C. *Geochim. Cosmochim. Acta* **64**, 2993–3005.

Newton R. C. and Manning C. E. (2002) Solubility of silica in equilibrium with enstatite, forsterite, and H_2O at deep crust/upper mantle pressures and temperatures and an activity-concentration model for polymerization of aqueous silica. *Geochim. Cosmochim. Acta* **66**, 4165–4176.

Newton R. C. and Manning C. E. (2003) Activity coefficient and polymerization of aqueous silica at 800 °C, 12 kbar, from solubility measurements on SiO_2-buffered assemblages. *Contrib. Mineral. Petrol.* **146**, 135–143.

Newton R. C. and Manning C. E. (2005) Solubility of anhydrite, $CaSO_4$, in NaCl–H_2O solutions at high pressures and temperatures: applications to fluid–rock interaction. *J. Petrol.* **46**, 701–716.

Newton R. C. and Manning C. E. (2006) Solubilities of corundum, wollastonite and quartz in H_2O–NaCl solutions at 800 °C and 10 kbar: interaction of simple minerals with brines at high pressure and temperature. *Geochim. Cosmochim. Acta* **70**, 5571–5582.

Pokrovskii V. A. and Helgeson H. C. (1995) Thermodynamic properties of aqueous species and the solubilities of minerals at high pressures and temperatures in the system Al_2O_3–H_2O-NaCl. *Am. J. Sci.* **295**, 1255–1342.

Rice J. M. (1983) Metamorphism of rodingites: Part I. Phase relations in a portion of the system CaO–MgO–Al_2O_3–SiO_2–CO_2–H_2O. *Am. J. Sci.*, 121–150.

Thompson A. B. (1975) Calc-silicate diffusion zones between marble and pelitic schist. *J. Petrol.* **16**, 314–346.

Tropper P. and Manning C. E. (2005) Very low solubility of rutile in H_2O at high pressure and temperature, and its implications for Ti mobility in subduction zones. *Am. Mineral.* **90**, 502–505.

Tropper P. and Manning C. E. (2007) The solubility of corundum in H_2O at high pressure and temperature and its implications for Al mobility in the deep crust and upper mantle. *Chem. Geol.* **240**, 54–60.

Walther J. V. (2001a) Experimental determination and analysis of the solubility of corundum in 0.1 and 0.5 m NaCl solutions between 400 and 600 °C from 0.5 to 2.0 kbar. *Geochim. Cosmochim. Acta* **65**, 2843–2851.

Walther J. V. (2001b) Experimental determination and analysis of the solubility of corundum in 0.1-molal $CaCl_2$ solutions between 400 and 600 °C from 0.6 to 2.0 kbar. *Geochim. Cosmochim. Acta* **66**, 1621–1626.

Warren R. G., Hensen B. J. and Ryburn R. J. (1987) Wollastonite and scapolite in Precambrian calc-silicate granulites from Australia and Antarctica. *J. Metamorph. Geol.* **5**, 213–223.

Westrum, Jr., W. F., Essene E. J. and Perkins, III, D. (1979) Thermophysical properties of the garnet grossular. *J. Chem. Thermodyn.* **11**, 57–66.

Yoder, Jr., H. S. (1950) Stability relations of grossularite. *J. Geol.* **58**, 221–253.

Associate editor: Thomas Chacko